Available online at www.sciencedirect.com
ScienceDirect
Physica E 40 (2008) 1364–1366
PHYSICA E
www.elsevier.com/locate/physe

The effect of inter-valley scattering on weak localisation in graphene

F.V. Tikhonenko*, D.W. Horsell, B. Wilkinson, R.V. Gorbachev, A.K. Savchenko

School of Physics, University of Exeter, Stocker Road, Exeter, EX4 4QL, UK

Available online 11 September 2007

Abstract

We experimentally demonstrate that weak localisation (WL) exists in graphene fabricated by mechanical exfoliation at different carrier densities. We show that it is controlled not only by inelastic dephasing mechanisms, but also by elastic intra- and inter-valley scattering. By reducing the width of the graphene sample, inter-valley scattering is found to be limited by the sample boundaries. Intravalley scattering, which suppresses WL in one valley, is found to be much faster than inter-valley scattering. In the Dirac point, where there is a zero-net carrier density, we observe a distinct change in both elastic and inelastic scattering.

PACS: 73.23.−b; 72.15.Rn; 73.43.Qt

Keywords: Weak localisation; Magnetoconductance; Graphene

1. Introduction

One of the simplest ways to observe directly the wave-like nature of electrons has been to measure the weak localisation (WL) correction to the conductivity of a two-dimensional conductor. Detailed analysis of this effect, originating from the interference of electrons on closed trajectories, has proved to be valuable way to extract information about the inelastic scattering mechanisms that underlie dephasing in charge transport. It has been shown [1,2] that WL in the recently discovered two-dimensional system, graphene [3], cannot only provide information about the dephasing but also elastic scattering mechanisms [4,5].

Elastic scattering in graphene occurs both within a single valley (intra-valley) and between valleys (inter-valley). It affects WL due to the pseudospin quantum number defining the carrier wavefunction in graphene—a result of the chiral property of the honeycomb crystal structure. The pseudospin behaves in a similar way to conventional spin in that it controls the phase of the wavefunction, and hence affects WL. The intra-valley effects that suppress WL are "chirality-breaking" scattering, which can occur off lattice dislocations and other topological defects [6,7], and the "trigonal warping" of the Fermi surface [4]. Inter-valley scattering, from atomically sharp defects, restores WL, both by allowing chirality-conserving scattering events to occur and by effectively symmetrizing the Fermi surface.

The WL correction to the conductivity of graphene is [4]

$$\delta\sigma(B) = \frac{e^2}{\pi\hbar}\left\{\mathscr{F}\left(\frac{B}{B_\phi}\right) - \mathscr{F}\left(\frac{B}{B_\phi + 2B_\mathrm{i}}\right) - 2\mathscr{F}\left(\frac{B}{B_\phi + B_\mathrm{i} + B_*}\right)\right\}, \quad (1)$$

where $\mathscr{F}(x) = \ln(x) + \Psi(\frac{1}{2} + 1/x)$, $B_{\phi,\mathrm{i},*} = (\hbar/4De)\tau^{-1}_{\phi,\mathrm{i},*}$, and the intravalley scattering rate $\tau_*^{-1} = \tau_\mathrm{w}^{-1} + \tau_z^{-1}$. Here τ_i^{-1} is the inter-valley scattering rate, τ_z^{-1} is the chirality-breaking, and τ_w^{-1} the trigonal-warping rates. At low fields we see experimentally a positive magnetoconductivity followed by a saturation or down-turn at higher fields, and thus we infer from Eq. (1) that both τ_i^{-1} and τ_*^{-1} are significant scattering rates in graphene.

In a system free from atomically sharp scatterers, τ_i^{-1} is necessarily limited by the physical boundaries of the graphene system, and τ_*^{-1} must have an upper limit of τ_p^{-1}. The momentum relaxation rate τ_p^{-1} is determined by impurities from the silica substrate [4] (i.e. a smooth potential) which does not affect the chirality.

*Corresponding author. Fax: +44 1392264111.
E-mail address: Fedor.Tikhonenko@exeter.ac.uk (F.V. Tikhonenko).

1386-9477/$ - see front matter © 2007 Elsevier B.V. All rights reserved.
doi:10.1016/j.physe.2007.09.010

2. Experiment

The graphene flakes were produced by the process of mechanical exfoliation [3]. They were deposited on an n^+ Si wafer coated with 300 nm SiO_2. Lithographically defined Au/Cr contacts were then made to each flake. The resistance of the devices was measured by a standard lock-in technique in the temperature range 0.25–20 K in a perpendicular magnetic field. We consider here two samples, B and F2: B is a long ribbon of length $L = 3.7\,\mu m$ and width $W = 0.3\,\mu m$; F2 is the same length as B, but wider with $W = 1.8\,\mu m$.

The resistivity of each sample as a function of carrier density (controlled by the gate voltage V_g) is shown in Fig. 1. The samples are sufficiently small such that reproducible mesoscopic fluctuations of the conductance occur in all ranges of carrier density. To analyse WL we average the data over a large number of these fluctuations ($\Delta V_g = 2\,V$) to suppress their influence [1].

A fit of Eq. (1) to the magnetoconductivity data of sample F2 shows excellent agreement for all carrier densities, including the Dirac region, Fig. 2. The lengths L_i and L_* ($L_x^2 = D\tau_x$, where D is the diffusion coefficient) extracted from the fit are T-independent over the whole temperature range. Also, we find for all densities that $L_i \gg L_*$. The inter-valley scattering length appears to be limited by the width of the sample, $L_i/W \sim 0.5$. In contrast, $L_* \gtrsim l$, the mean free path, and is therefore not controlled by the same mechanisms as the inter-valley scattering. This argument is strengthened when it is seen that in the Dirac point L_i is suppressed whereas L_* is enhanced, Fig. 2(a).

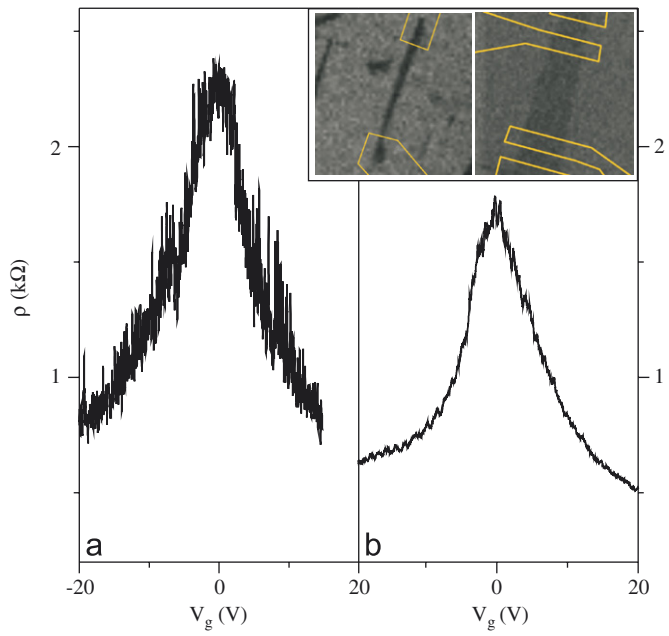

Fig. 1. Resistivity of samples B1 (a) and F2 (b) at $T = 0.25\,K$ as a function of carrier density. The inset shows electron micrographs of sample B1 (left) and F2 (right) with the positions of the contacts shown as outlines.

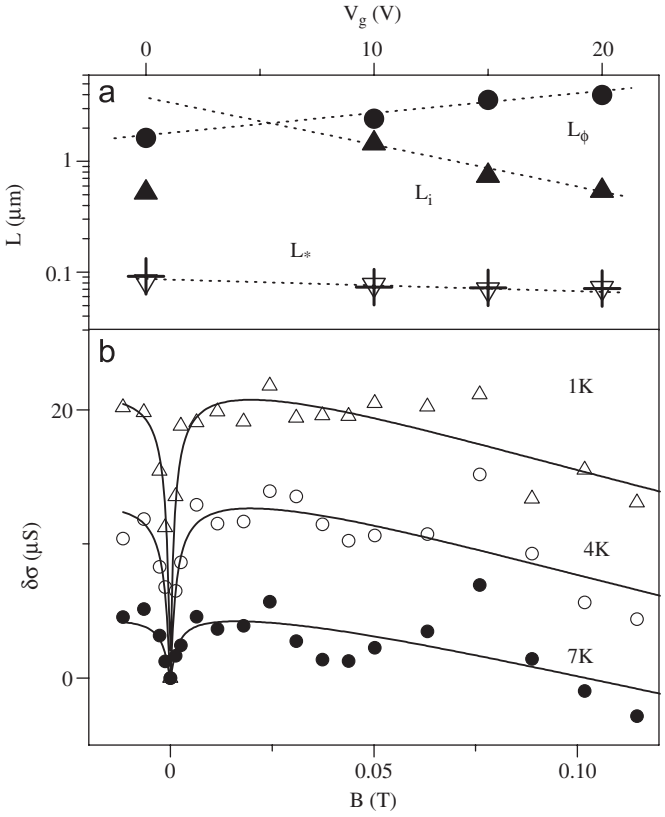

Fig. 2. Weak localisation in sample F2. (a) Dependence of characteristic lengths on carrier density (the value of L_φ is the saturation value at low temperatures). The dotted lines are guides to the eye. The crosses show the corresponding values of l. (b) Examples of the fit (solid lines) of the magnetoconductivity data (symbols) at high carrier density ($V_g = 10\,V$) to Eq. (1).

The dephasing length L_φ is also affected by the geometry of the sample at low temperatures as the sample boundaries limit the size of the trajectories that can contribute to WL. The temperature dependence of L_φ is seen to be significantly suppressed for $T < 3\,K$ as these geometric limits are approached. (The high temperature data are discussed elsewhere [2].)

The magnetoconductivity of sample B has a significantly different shape to that of F2, Fig. 3. As the zero-field conductivity (and hence mean free path and diffusion coefficient) are comparable, L_φ in both samples should also be of similar size; this is seen experimentally, Fig. 3(a). The very strong WL correction in B (Fig. 3(b)), which shows less saturation and no downturn, must therefore be the result of fast inter-valley scattering. As L_i is limited by the width in sample F2, we can expect a much smaller value of $L_i \sim 0.1-0.2\,\mu m$ in sample B. However, to make the comparison we must be sure we are dealing with 2D and not 1D WL due to the small width of sample B.

For 1D WL analysis we must satisfy the condition $W \ll L_\varphi$ [4], and $B \ll \hbar/eW^2 \sim 7\,mT$. If we attempt to fit the 1D expression, $\delta\sigma_{1D} = -2e^2 L_\varphi/h(1+(\tau_B^{-2}/3\tau_\varphi^{-1}\tau_W^{-1})^{-1/2} - 1)$, where $\tau_W^{-1} = D/W^2$ and assuming that $L_i \to 0$, we find good agreement even for much stronger fields, Fig. 3(b). Indeed, if we allow W as a free fitting parameter we find

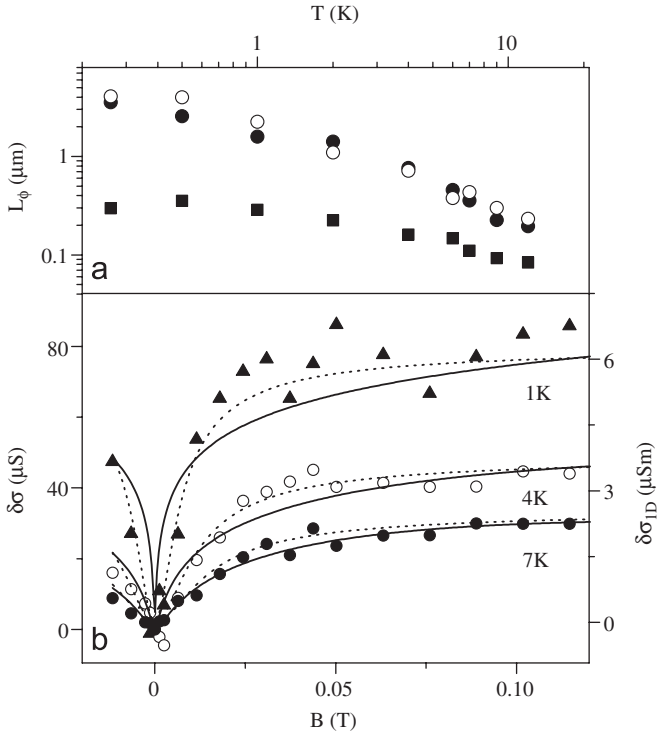

Fig. 3. Weak localisation in sample B. (a) $L_\varphi(T)$ for electron (solid circles), hole (open circles), and Dirac (squares) regions. (b) Examples of the fit (solid lines) of the magnetoconductivity data (symbols) at high carrier density to Eq. (1). The dashed lines show the corresponding fits in the 1D approximation.

the best fit to the equation gives $W = 0.24 \pm 0.05\,\mu\text{m}$ (for $T < 5\,\text{K}$), agreeing well with the geometric width. However, the validity of this 1D analysis is questionable: not only is the field limit exceeded, but also extending the formula to include finite L_i and L_* results in values $\lesssim l/10$, which are unrealistic.

We now return to the analysis of WL in sample B in terms of Eq. (1). As expected, L_i and L_* are found to be small ($\sim$100 nm) and comparable to the mean free path at all concentrations. In contrast, L_φ is close to that seen in sample F2. Also, like F2, the dephasing length is significantly reduced in the Dirac region. From Eq. (1) we see that the condition $\tau_\text{i}^{-1} \sim \tau_*^{-1} \gg \tau_\varphi^{-1}$ destroys the last two terms in the expression leading to conventional WL, without a downturn in the magnetoconductivity.

3. Discussion

The WL correction near the Dirac point is seen to be different from that at high carrier density. For sample F2 this equates to the dephasing length being shortened by $\sim$40%. This can be due to the onset of inhomogeneity in the graphene flake that breaks the Fermi sea into a mosaic of electron–hole puddles [2]. In B the difference in L_φ between the Dirac region and higher densities is more pronounced. One can see that the dephasing length is reduced in this region by more than a factor of three accompanied by little or no change in L_i or L_*. The onset of inhomogeneity in the narrow sample thus appears to have a much more dramatic effect on the interference.

In both samples, L_* tends to approach the mean free path. The decrease in L_* with increasing carrier density seen in F2 suggests that trigonal-warping, rather than chirality-breaking, can be the main source of intra-valley scattering: it is expected that $\tau_\text{w}^{-1} \propto \tau_\text{p} n^2$ [4]. However, rough estimation shows that trigonal-warping is too weak to account for such a small L_*. Intra-valley scattering thus has a topological origin and can be the result of ripples or dislocations in the graphene layer. Since $L_\text{i} \sim W \gg L_*$ in this sample, the origin cannot lie in atomically sharp scatterers within the layer or the sample boundaries. (The reason for the enhancement of inter-valley scattering and slight suppression of intra-valley scattering in the Dirac region of sample F2 is unclear, but also indicates that the inter- and intra-valley scattering mechanisms are different.)

In sample B the difference between L_i and L_* is much smaller. For this sample $L_\text{i}/W \sim 0.3$, from which we conclude that inter-valley scattering occurs off both the sample boundaries and additional sharp scatterers in the bulk. (We have identified these scatterers as pronounced ridges that extend across the sample width [2]. A small value of L_i with respect to the system size is also seen in Ref. [8], which can be attributed to additional scattering in the bulk.) The same scattering events can also break chirality, and this can account for the similar values of L_i and L_* seen in the experiment.

4. Conclusion

We have shown that WL occurs in graphene systems at all carrier densities, including the Dirac region where the net carrier density is zero. The intra- and inter-valley scattering were shown to affect the WL by causing a saturation and downturn of its magnetic field dependence. Inter-valley scattering is limited by the width of the graphene system. Intra-valley scattering is shown to have a topological origin and in a narrow sample can also be affected by the width. An increase of the dephasing rate in the Dirac region seen by the WL indicates an onset of inhomogeneity in graphene conduction in this region.

References

[1] R.V. Gorbachev, F.V. Tikhonenko, A.S. Mayorov, D.W. Horsell, A.K. Savchenko, Phys. Rev. Lett. 98 (2007) 176805.
[2] F.V. Tikhonenko, D.W. Horsell, R.V. Gorbachev, A.K. Savchenko, arXiv:0707.0140.
[3] K.S. Novoselov, A.K. Geim, S.V. Morozov, D. Jiang, Y. Zhang, S.V. Dubonos, I.V. Grigorieva, A.A. Firsov, Science 306 (2004) 666.
[4] E. McCann, K. Kechedzhi, V.I. Fal'ko, H. Suzuura, T. Ando, B.L. Altshuler, Phys. Rev. Lett. 97 (2006) 146805.
[5] K. Kechedzhi, V.I. Fal'ko, E. McCann, B.L. Altshuler, Phys. Rev. Lett. 98 (2007) 176806.
[6] A.F. Morpurgo, F. Guinea, Phys. Rev. Lett. 97 (2006) 196804.
[7] S.V. Morozov, et al., Phys. Rev. Lett. 97 (2006) 016801.
[8] X. Wu, X. Li, Z. Song, C. Berger, W.A. de Heer, Phys. Rev. Lett. 98 (2007) 136801.